İSTANBUL TİCARET ÜNİVERSİTESI
FEN BİLİMLERİ DERGİSİ

İstanbul Commerce University Journal of Science

http://dergipark.org.tr/ticaretfbd

REVISITING MODE CONVERSION BETWEEN TRANSMISSION LINES FOR WIDE-BAND MODELING OF DEFECTED GROUND STRUCTURES

KUSURLU TOPRAK YAPILARININ GENİŞ BANTLI MODELLENMESI İÇIN İLETİM HATLARI ARASINDAKI MOD DÖNÜŞÜMÜNÜN TEKRAR İNCELENMESI

Seyit Ahmet SİS[1]   **Fatih ÜSTÜNER**[2]

https://doi.org/10.55071/ticaretfbd.1245842

Corresponding Author / Sorumlu Yazar
fustuner@ticaret.edu.tr

Abstract

This paper presents a wide-band transmission line model for defected ground structures (DGSs) based on a mode-conversion between microstrip- and slot-lines. The defects on the ground plane are modeled as short- or open-ended transmission lines (TLs) with slot-line characteristics. The transition between microstrip line and ground defect is modeled with interdependent voltage and current sources, of which the first one is placed in series with the microstrip line, and the latter in-shunt with the slot lines, respectively. A complete set of geometry-dependent analytical expressions for the ABCD parameter of a two-port microstrip line crossing over the defected structure is provided. Therefore, the proposed model can be readily integrated into computer-aided design programs. The model's accuracy is verified in various defect shapes by comparing its results with those from HFSS simulations and measurements.

Keywords: Defected ground structure (DGS), DGS Modeling, circuit model, microstrip line, mode-conversion, wide-band model, slot-line.

Öz

Bu makale, kusurlu toprak yapıları (DGS'ler) için mikroşerit ve yarık hatlar arasında mod dönüşümüne dayanan bir geniş bantlı iletim hattı modeli sunmaktadır. Toprak düzlemindeki kusurlar, yarıklı hat (slot-line) özelliklerine sahip kısa veya açık devre ile sonlandırılmış iletim hatları (İH'ler) olarak modellenmiştir. Mikroşerit hat ile topraklama kusuru arasındaki geçiş, sırasıyla ilki mikroşerit hat ile seri ve ikincisi yarık hatlarla şönt olarak yerleştirilmiş birbirine bağlı gerilim ve akım kaynakları ile modellenmiştir. Önerilen modelde kusurlu yapı üzerinden geçen iki portlu bir mikroşerit hattın tüm ABCD parametresi geometriye bağlı bir analitik ifadeler seti sağlanmaktadır. Bu da, önerilen modelin bilgisayar destekli tasarım programlarına kolayca entegre edilebilmesine olanak sağlamaktadır. Modelin doğruluğu, model sonuçlarının HFSS simülasyonları ve ölçümlerinden alınan sonuçlarla karşılaştırılarak çeşitli kusur şekilleri için doğrulanmıştır.

Anahtar Kelimeler: Devre modeli, geniş bant modeli, DGS modelleme, kusurlu toprak yapısı (DGS), mikroşerit hattı, mod dönüştürme, yarıklı hat.

[1]Balikesir University, Faculty of Engineering, Department of Electrical and Electronics Engineering, Cagis Campus, Balikesir, Türkiye.
seyit.sis@balikesir.edu.tr, Orcid.org/0000-0002-3740-2391.

[2]İstanbul Commerce University, Faculty of Engineering, Department of Electrical and Electronics Engineering, İstanbul, Türkiye.
fustuner@ticaret.edu.tr, Orcid.org/0000-0001-9968-5123.

1. INTRODUCTION

Thanks to their compact size and ease of implementation, defected ground structures (DGSs) find their utilization in almost all types of microwave circuits including, amplifiers, filters, oscillators, and antennas (Jahan et al., 2020; Jong-Sik Lim et al., 2001; Khalid et al., 2020; Luo et al., 2018; Wei et al., 2017; Zhong et al., 2017). An accurate analytical model for the DGS is a major demand for microwave circuit designers; therefore, various circuit models are proposed (Ahn et al., 2001; Caloz et al., 2004; Challal et al., 2016; Chul-Soo Kim et al., 2002; Jun-Seok Park et al., 2002; Karmakar et al., 2006; Khandelwal et al., 2017; Knorr, 1974; Park et al., 2005; Sis et al., 2022; van Nechel et al., 2019; Woo et al., 2013). A parallel LC resonator produces the same electrical response as that of DGS (Ahn et al., 2001; Khandelwal et al., 2017; Woo et al., 2013). This simple model is useful for characterizing the DGS for a given electrical response; however, its narrowband response makes this model valid near the fundamental resonance frequency of the DGS. For wideband modeling, multiple cascaded LC circuits are proposed for representing higher-order resonances as well (van Nechel et al., 2019). Nevertheless, both models do not possess expressions relating the circuit geometry to its lumped element values; therefore, they are not quite useful for predicting the circuit's response in the initial design stage.

Other more complex lumped element models are also proposed in the literature (Jun-Seok Park et al., 2002; Karmakar et al., 2006; Khandelwal et al., 2017). The π-shaped lumped model in (Jun-Seok Park et al., n.d.) is a slightly modified version of the LC model with extra shunt-connected RC branches on both sides of the series-connected parallel LC resonator. These extra RC components provide the model to represent phase variation as well and yield more accurate results (Jun-Seok Park et al., 2002; Khandelwal et al., 2017). This model, however, also does not provide a direct relationship between the geometry of the circuit and the lumped element values. The quasi-static model (Karmakar et al., 2006) overcomes the aforementioned limitation by providing model parameters as a function of the physical dimensions of the DGS. Yet this model represents DGS near its fundamental resonance frequency and seems not to be accurate in wideband simulations.

The transmission line (TL)-based models are inherently suitable for wide-band modeling of distributed circuits; therefore various circuits are proposed for modeling DGSs (Caloz et al., 2004; Challal et al., 2016; Chul-Soo Kim et al., 2002; Das, 1993; Knorr, 1974; Park et al., 2005; Sis et al., 2022). In the TL-based models, the defects on the ground plane are usually represented by ideal TLs with slot-line characteristics (Caloz et al., 2004; Challal et al., 2016; Park et al., 2005), hence, these ideal TLs exhibit repeating resonance frequencies, which are observed in the frequency response of real DGS-based circuits. In these models, usually, the transition between the microstrip line and the defect is represented by an ideal transformer.

A TL model, based on a mode-conversion between the microstrip line and slot-line, was reported a while ago, even before the concept of DGS was not well-defined, for use in modeling signal integrity issues at the split ground planes (Haw-Jyh Liaw & Merkelo, 1996). In this mode-conversion-based transmission line (MCTL) model, the signal transition between microstrip and slot-line transmission lines is represented by interdependent voltage and current sources rather than transformers, which provide more physical insight than modeling through inductive coupling via transformers.

This paper revisits the mode conversion technique between transmission lines and proposes a wide band TL model for use in defected ground structures. Complete analytical expressions are derived as a function of the physical dimensions of DGS, making the model suitable to be readily utilized in a CAD software. The accuracy of the model is verified in various DGS shapes for wide frequency bands by comparing the model's results with those from HFSS (Ansys, H. F. S. S. "Ansys Inc.," 1998) simulations and measurements.

2. MODE CONVERSION-BASED TL MODEL FOR DGSs

A typical DGS structure and the schematic of the mode conversion-based transmission line (MCTL) model are shown in Fig. 1 (a) and (b), respectively. TL models for the microstrip line and slot-line on the ground defect are shown in two different dashed boxes and the signal in these two transmission line modes are converted to one another through dependent voltage and current sources as shown in Fig. 1 (b). The return current of the microstrip line on the ground plane is split into two halves by the defect and converted into the slot-line current, which is represented by the dependent current source I_{sl} in the model as shown in Fig. 1 (b).
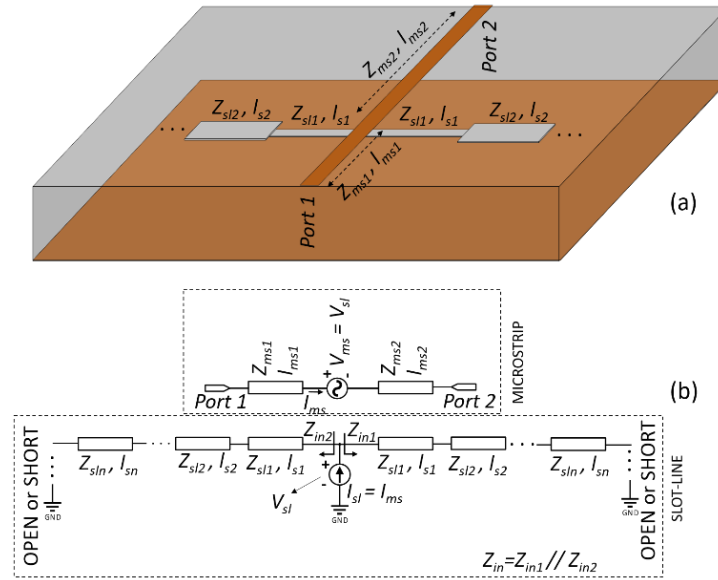

Figure 1. (a) A typical DGS structure and (b) schematic of the MCTL model for a typical DGS structure.

Since the I_{sl} is the return of the current passing through the microstrip line, I_{ms}, it is dependent and equal to the I_{ms}. The voltage seen across the slot-line, V_{sl}, is essentially the voltage seen on the dependent current source (I_{sl}) as seen in Fig 1 (b), and is formed as follows:

$$V_{sl} = I_{sl} \cdot Z_{in} \tag{1}$$

where Z_{in} is the parallel of the impedances seen towards both halves of the slot-line ($Z_{in}=Z_{in1}//Z_{in2}$). The V_{sl} rules the value of the dependent voltage source, V_{ms}, placed between the two halves of the microstrip line (Fig. 1 (b)). This way, the effect of introduced impedance due to the slot-line on the ground plane (Z_{in}) is simply reflected in the microstrip part of the model as shown in Fig. 1 (b). In the model, the Z_{ms1}, Z_{ms2} and l_{ms1}, l_{ms2} are characteristic impedances and lengths for the microstrip lines, respectively. Similarly, the $Z_{sl1},…Z_{sln}$, and $l_{s1},…l_{sn}$ are characteristic impedances and lengths for the slot lines, respectively. The impedances Z_{in1} and Z_{in2} are the input impedances of the cascaded ideal slot-line transmission lines on both sides of the dependent current source as shown in Fig. 1 (b). The ends of each half of slot lines may be short or open, respectively. Analytical expressions for Z_{in1} and Z_{in2} depend on the configuration of the cascaded slot-line structure. To illustrate this, four different configurations of slot-line defects on the ground plane are considered as shown in Fig. 2 (a)-(d).
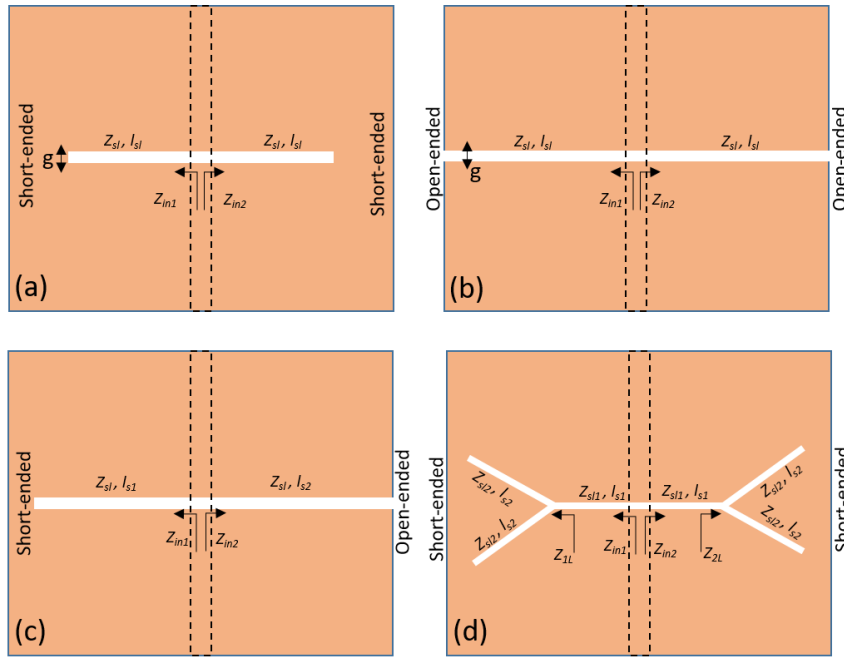
Figure 2. A top view of four different configurations of slot-line defects on the ground plane: (a), (b) a uniform slot line with constant width throughout the whole defect with short (configuration 1) and open (configuration 2) ends, respectively, (c) a uniform slot with asymmetric placement (configuration 3), and (d) a V-type branched slot line defect (configuration 4).

The first two configurations (Fig. 2 (a) and (b)) employ slots that are symmetrically divided under the microstrip line, and the slots are short- and open-ended in these configurations, respectively. The third configuration (Fig. 2 (c)) employs an asymmetrically divided slot in which one edge is ended with an open and the other edge is ended with a short circuit. The last configuration (Fig. 2 (d)) employs V-type branched slots, which are also symmetrically divided under the microstrip line. For the uniform slot structure with a constant width over the whole defect, as seen in Fig. 2 (a)-(b), the Z_{in1} and Z_{in2} are simply as follows for the short-ended slot line (Fig. 2 (a)):

$$Z_{in1,2} = jZ_{sl} \tan(\beta_{sl} l_{sl}) \tag{2}$$

and for the open-ended slot-line (Fig. 2 (b)):

$$Z_{in1,2} = -jZ_{sl} \cot(\beta_{sl} l_{sl}) \tag{3}$$

respectively (Pozar, 2011). In (2) and (3), the Z_{sl}, l_{sl} and β_{s1} are the characteristic impedance, length, and wave-constant for the slot structure, respectively. The characteristic impedance of a slot-line (Z_{sl}) as a function of its physical dimensions is as follows (Janaswamy & Schaubert, 1986) :

$$Z_{sl} = 60 + 3.69 \sin\left[\frac{(\varepsilon_r - 2.22)\pi}{2.36}\right] + 133.5 \ln(10\varepsilon_r)\sqrt{g/\lambda_0}$$
$$+ 2.81\left[1 - 0.011\varepsilon_r(4.48 + \ln(\varepsilon_r))\right](g/d)\ln(100d/\lambda_0)$$
$$+ 131.1(1.028 - \ln(\varepsilon_r))\sqrt{d/\lambda_0}$$
$$+ 12.48(1 + 0.18\ln(\varepsilon_r))\frac{g/d}{\sqrt{\varepsilon_r - 2.06 + 0.85(g/d)^2}}$$
(4)

where ε_r, λ_0, d, and g are the relative permittivity of the dielectric layer, the wavelength at free space, the thickness of the dielectric layer, and the width of the slot, respectively. The expression of Z_{sl} in (4) is valid for $2.22 < \varepsilon_r < 3.8$ and $0.0015 < g/\lambda_0 < 0.075$. The effective dielectric constant of the slot line (ε_{eff}) is as follows (Janaswamy & Schaubert, 1986):

$$\varepsilon_{eff} = (\frac{\lambda_0}{\lambda_s})^2$$
(5)

where the slot-line wavelength (λ_s) is as follows:

$$\lambda_s = 1.045\lambda_0 - 0.365\ln(\varepsilon_r)\lambda_0 + \left[\frac{6.3(g/d)\varepsilon_r^{0.945}}{238.64 + 100g/d}\right]\lambda_0$$
$$- \left[\left[0.148 - \frac{8.81(\varepsilon_r + 0.95)}{100\varepsilon_r}\right]\ln(d/\lambda_0)\right]\lambda_0$$
(6)

The Z_{in1} and Z_{in2} for the third configuration, shown in Fig. 2 (c), can be obtained using the transmission-line impedance equation as follows (Pozar, 2011):

$$Z_{in1} = jZ_{sl1}\tan(\beta_{sl1}l_{sl1})$$
(7)

and

$$Z_{in2} = -jZ_{sl2}\cot(\beta_{sl2}l_{sl2})$$
(8)

Since the short-ended slot lines on the V-type branches in the last configuration (Fig 2 (d)) are electrically-connected in series, the Z_{1L} and Z_{2L} are as follows:

$$Z_{1,2L} = 2jZ_{sl2}\tan(\beta_{sl2}l_{s2})$$
(9)

Then the Z_{in1} and Z_{in2} for the fourth configuration, shown in Fig. 2 (d), can be obtained using the transmission-line impedance equation as follows (Pozar, 2011):

$$Z_{in1,2} = Z_{sl}\frac{Z_{1,2L} + jZ_{sl}\tan(\beta_{sl}l_{s1,2})}{Z_{sl} + jZ_{1,2L}\tan(\beta_{sl}l_{s1,2})}$$
(10)

Once the parallel impedances, Z_{in1} and Z_{in2}, are calculated, then the total input impedance seen towards the defect, Z_{in}, is as follows:

$$Z_{in} = Z_{in1} // Z_{in2} \tag{11}$$

The characteristic impedances of slot lines used in the above equations, Z_{sl1} and Z_{sl2} (see Fig 2 (c) and (d)), can also be calculated using (4). It should be noted that the above-given configurations in Fig. 2 are just four examples of many different defect shapes presented in the literature. The MCTL model discussed in this work is not limited to those four configurations but can be readily utilized for all defect configurations by applying the basic transmission-line theory. Once the input impedances of the defect (Z_{in}) is calculated for all four configurations using (2)-(10), then the two-port network parameters of the MCTL model in Fig. 1 (b) can be extracted by first treating the microstrip part of the model as three separate cascaded networks as shown in Fig. 3.
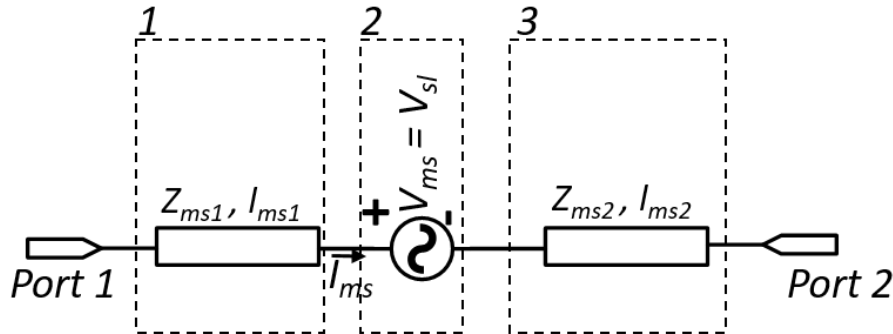

Figure 3. The three-cascaded sections of the microstrip part in the MCTL model.

The total ABCD parameter of this two-port network is the matrix multiplication of the ABCD parameters of each network as follows:

$$
\begin{bmatrix} A & B \\ C & D \end{bmatrix} = \begin{bmatrix} \cos(\beta_{ms1}l_{ms1}) & jZ_{ms1}\sin(\beta_{ms1}l_{ms1}) \\ j\dfrac{1}{Z_{ms1}}\sin(\beta_{ms1}l_{ms1}) & \cos(\beta_{ms1}l_{ms1}) \end{bmatrix}
$$
$$
\cdot \begin{bmatrix} 1 & Z_{in} \\ 0 & 1 \end{bmatrix} \cdot \begin{bmatrix} \cos(\beta_{ms2}l_{ms2}) & jZ_{ms2}\sin(\beta_{ms2}l_{ms2}) \\ j\dfrac{1}{Z_{ms2}}\sin(\beta_{ms2}l_{ms2}) & \cos(\beta_{ms2}l_{ms2}) \end{bmatrix}. \tag{12}
$$

where β_{ms1} and β_{ms2} are the wave constants for the microstrip transmission lines. The characteristic impedance of microstrip transmission-line sections, Z_{ms1} and Z_{ms2}, are calculated using the expressions given in (Pozar, 2011).

3. ELECTROMAGNETIC SIMULATIONS AND MEASUREMENT RESULTS

The MCTL model is verified by comparing its results with those from measurement and electromagnetic (EM) simulation results on four different circuit configurations, which are exactly the same as in Fig. 2. The physical dimensions of the realized circuits are detailed in Table I. A Rogers' 4003C ceramic laminate with a dielectric thickness, conductor thickness and relative permittivity (ε_r) of 0.508 mm, 35 μm and 3.55, respectively, is utilized as a substrate. In all these four configurations, microstrip line width is chosen as 1.096 mm to achieve a 50 Ω characteristic impedance for the aforementioned substrate properties. The EM simulations are performed in

high-frequency structure simulator (HFSS) and its' full two-port scattering parameters (S-parameters), for 50 Ω port impedance, are obtained within a frequency range of 100 MHz – 6 GHz. The two-port scattering parameters (S-parameters) of the fabricated circuits are measured using an Agilent PNA series E8362B network analyser with a 50-Ω system impedance.

Table 1. Physical Dimensions of the Circuits Used in Verification of the Model

Conf.	Slot width (g)	Slot Length (l_{sl})*	Microstrip line Width (W)	Microstrip line length (l_{ms})
1	0.5 mm	50 mm	1.096 mm	95.7 mm
2	0.5 mm	75 mm	1.096 mm	95.7 mm
3	0.5 mm	l_{sl1}=35.5 mm, l_{sl2}=37.5 mm	1.096 mm	47.6 mm
4	g_1=0.5 mm g_2=0.5 mm	l_{sl1}=10.5 mm, l_{sl2}=10.5 mm	1.096 mm	47.6 mm

The defect length is twice the length of the slot length (l_{sl}) given in the Table. That is, the l_{sl} is defined as half of the total defect length (see Fig. 2).

Fig. 4 (a)-(d) shows a comparison of the MCTL model's results with those from EM simulations and measurement results for configurations 1-4, respectively. As seen in Fig. 4 (a) and (b), a very good agreement is achieved between these three results in frequency range of 100 MHz to 6 GHz. Since configuration 2 has a longer slot length, it creates larger number of resonance dips in measured frequency range (Fig. 4 (b)). Having a short-ended load for the slot line in configuration 1 causes a low-pass filter response at low frequencies (Fig. 4 (a)). On the other hand, having an open-ended load for the slot line in configuration 2 causes a transmission zero at DC (Fig. 4 (b)). Fig. 4 (c) shows comparison of the MCTL model's results with those from EM simulations and measurement results for configuration 3. As seen in Fig. 4 (c), the asymmetric placement and different ending of the slots on each side causes slight deviation between MCTL model, HFSS and simulation results. Finally, Fig. 4 (d) shows the same comparison for the fourth configuration. A good agreement is achieved between MCTL model, HFSS and simulation results.
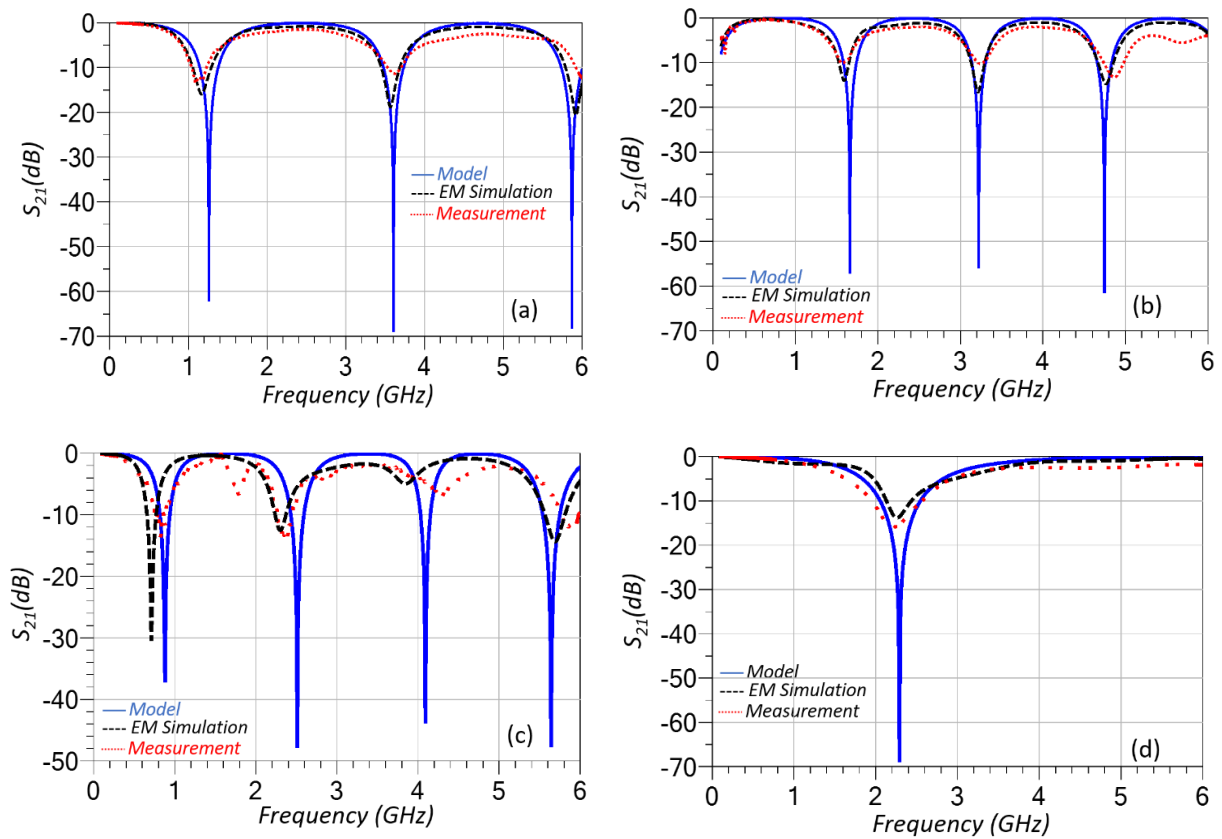
Figure 4. Comparison of the MCTL model's results with those from EM simulation and measurement for (a) configuration 1, (b) configuration 2, (c) configuration 3 and (d) configuration 4.

It should be noted that the MCTL model here is limited only to typical slot structures as in four configurations shown in Figure 2. In case of employing complex defects such as meandered slots exhibiting slow-wave effect, and sharp discontinuities, the MCTL model should be modified to include those effects.

4. CONCLUSION

In this paper, a wide-band MCTL model, originally utilized for modeling the discontinuities on the split ground planes is applied to defected ground structures successfully. The model's accuracy is verified through the HFSS simulations and measurement results of four circuits with different defect configurations. Complete analytical expressions for the two-port model presented in this work can be readily incorporated into an RF circuit simulator. Since the model is a distributed element model built on transmission line theory, any structural modifications on both the slot and the microstrip line can simply be incorporated into the modeling of the corresponding transmission line.

Contribution of The Authors
The authors confirm that they equally contributed to this paper.

Conflict of Interest
There is no conflict of interest between the authors.

Statement of Research and Publication Ethics
Research and publication ethics were observed in the study.

REFERENCES

Ahn, D., Park, J.-S., Kim, C.-S., Kim, J., Qian, Y., & Itoh, T. (2001). A design of the low-pass filter using the novel microstrip defected ground structure. *IEEE Transactions on Microwave Theory and Techniques*, 49(1), 86–93. https://doi.org/10.1109/22.899965

Ansys, (1998). H. F. S. S. *"Ansys Inc."*

Caloz, C., Okabe, H., Iwai, T., & Itoh, T. (2004). A simple and accurate model for microstrip structures with slotted ground plane. *IEEE Microwave and Wireless Components Letters*, 14(3), 127–129. https://doi.org/10.1109/LMWC.2003.822564

Challal, M., Dehmas, M., Azrar, A., Aksas, R., & Trabelsi, M. (2016). Circuit modeling and EM simulation verification of DGS based low-pass filter employing transmission line model along with microstrip-slotline transitions. *MATEC Web of Conferences*, *52*, 01003. https://doi.org/10.1051/matecconf/20165201003

Chul-Soo Kim, Jong-Sik Lim, Sangwook Nam, Kwang-Yong Kang, Jong-Im Park, Geun-Young Kim, & Dal Ahn. (2002, June, 2-7). *The equivalent circuit modeling of defected ground structure with spiral shape.* IEEE MTT-S International Microwave Symposium Digest (Cat. No.02CH37278), 2125–2128. https://doi.org/10.1109/MWSYM.2002.1012290

Das, N. K. (1993). Generalized multiport reciprocity analysis of surface-to-surface transitions between multiple printed transmission lines. *IEEE Transactions on Microwave Theory and Techniques*, 41(6), 1164–1177. https://doi.org/10.1109/22.238542

Haw-Jyh Liaw, & Merkelo, H. (1996, May, 28-31). *Signal integrity issues at split ground and power planes.* Proceedings 46th Electronic Components and Technology Conference, 752–755. https://doi.org/10.1109/ECTC.1996.550491

Jahan, N., Baichuan, C., Barakat, A., & Pokharel, R. K. (2020). Utilization of Multi-Resonant Defected Ground Structure Resonators in the Oscillator Feedback for Phase Noise Reduction of K-Band VCOs in 0.18-μ m CMOS Technology. *IEEE Transactions on Circuits and Systems I: Regular Papers*, 67(4), 1115–1125. https://doi.org/10.1109/TCSI.2020.2965007

Janaswamy, R., & Schaubert, D. H. (1986). Characteristic Impedance of a Wide Slotline on Low-Permittivity Substrates (Short Paper). *IEEE Transactions on Microwave Theory and Techniques*, *34*(8), 900–902. https://doi.org/10.1109/TMTT.1986.1133465

Jong-Sik Lim, Ho-Sup Kim, Jun-Seek Park, Dal Ahn, & Sangwook Nam. (2001). A power amplifier with efficiency improved using defected ground structure. *IEEE Microwave and Wireless Components Letters*, *11*(4), 170–172. https://doi.org/10.1109/7260.916333

Jun-Seok Park, Jae-Ho Kim, Jong-Hun Lee, Sang-Hyuk Kim, & Sung-Ho Myung. (2002, June, 02-07). *A novel equivalent circuit and modeling method for defected ground structure and its application to optimization of a DGS lowpass filter.* IEEE MTT-S International Microwave Symposium Digest (Cat. No.02CH37278), 417–420. https://doi.org/10.1109/MWSYM.2002.1011644

Karmakar, N. C., Roy, S. M., & Balbin, I. (2006). Quasi-static modeling of defected ground structure. *IEEE Transactions on Microwave Theory and Techniques*, 54(5), 2160–2168. https://doi.org/10.1109/TMTT.2006.873633

Khalid, M., Iffat Naqvi, S., Hussain, N., Rahman, M., Fawad, Mirjavadi, S. S., Khan, M. J., & Amin, Y. (2020). 4-Port MIMO Antenna with Defected Ground Structure for 5G Millimeter Wave Applications. *Electronics*, 9(1), 71. https://doi.org/10.3390/electronics9010071

Khandelwal, M. K., Kanaujia, B. K., & Kumar, S. (2017). Defected Ground Structure: Fundamentals, Analysis, and Applications in Modern Wireless Trends. *International Journal of Antennas and Propagation*, *2017*, 1–22. https://doi.org/10.1155/2017/2018527

Knorr, J. B. (1974). Slot-Line Transitions (Short Papers). *IEEE Transactions on Microwave Theory and Techniques*, 22(5), 548–554. https://doi.org/10.1109/TMTT.1974.1128278

Luo, J., He, J., Wang, H., Chang, S., Huang, Q., & Yu, X.-P. (2018). A 28 GHz LNA using defected ground structure for 5G application. *Microwave and Optical Technology Letters*, 60(5), 1067–1072. https://doi.org/10.1002/mop.31112

Park, J., Park, K., Chang, S., & Ahn, D. (2005, February, 13-15). A New Equivalent Transmission Line Modeling of Dumbbell Type Defected Ground Structure. *Proceedings of the 4th WSEAS International Conference on Electronics, Hardware, Wireless and Optical Communications*. Salzburg Austria, 1-5.

Pozar, D. M. (2011). Microwave Engineering (4th ed.). *John wiley & sons*, USA.

Sis, S. A., Ustuner, F., & Demirel, E. (2022). EMI Reducing Interdigital Slot on Reference Planes of the PCBs. *IEEE Transactions on Electromagnetic Compatibility*, *64*(1), 219–229. https://doi.org/10.1109/TEMC.2021.3083654

Van Nechel, E., Ferranti, F., Rolain, Y., & Lataire, J. (2019, June, 18-21). A Wide-Band Equivalent Circuit Model for Single Slot Defected Ground Structures. *IEEE 23rd Workshop on Signal and Power Integrity (SPI)*, 1–3. https://doi.org/10.1109/SaPIW.2019.8781651

Wei, K., Li, J. Y., Wang, L., Xu, R., & Xing, Z. J. (2017). A new technique to design circularly polarized microstrip antenna by fractal defected ground structure. *IEEE Transactions on Antennas and Propagation*, *65*(7), 3721–3725. https://doi.org/10.1109/TAP.2017.2700226

Woo, D.-J., Lee, T.-K., & Lee, J. W. (2013). Equivalent circuit model for a simple slot-shaped DGS microstrip line. *IEEE Microwave and Wireless Components Letters*, *23*(9), 447–449. https://doi.org/10.1109/LMWC.2013.2274037

Zhong, Y., Yang, Y., Zhu, X., Dutkiewicz, E., Shum, K. M., & Xue, Q. (2017). An on-chip bandpass filter using a broadside-coupled meander line resonator with a defected-ground structure. *IEEE Electron Device Letters*, *38*(5), 626–629. https://doi.org/10.1109/LED.2017.2690283